West core radiative collapse modelling with RAPTOR

Ostuni V., Morales J., Artaud J-F, Bourdelle C., Manas P., Peysson Y., Fedorczak N., Dumont R., Goniche M., Maget P.

West core radiative collapse modelling with RAPTOR

DE LA RECHERCHE À L'INDUSTRIE

AAPPS 10/10/2022

V. Ostuni, J. Morales, J-F Artaud, C. Bourdelle, P. Manas, Y. Peysson, N. Fedorczak, R. Dumont, M. Goniche, P. Maget & WEST team

Outline

- Context;
- **Characterize** and **understand** the dynamics of the **radiative collapse** observed in WEST operation;
- **Reproduce** the rapid **collapse** of **central temperature** using an integrated model framework to **understand** which are the **actuators** that lead to the observed dynamics;
- Conclusions.

Outline

- **Context;**
- Characterize and understand the dynamics of the radiative collapse observed in WEST operation;
- Reproduce the rapid collapse of central temperature using an integrated model framework to understand which are the actuators that lead to the observed dynamics;
- Conclusions.

WEST: superconducting full W environment heated by RF

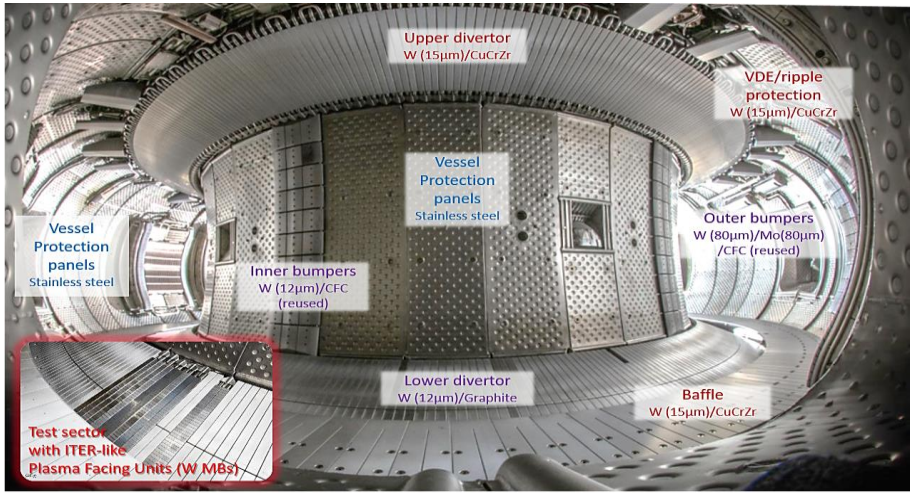

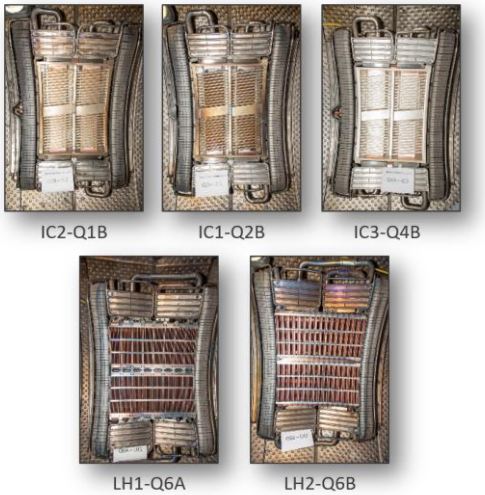

Designed for testing actively cooled ITER-like PFU

Phase I completed: with lower divertor equipped [Bucalossi NF 2022]

Here we will report on Phase I experiments where LHCD heating dominated.

B_T	3.7 T
R	2.5 m
a	0.4/0.5 m

Plateau Statistics Reduced L-mode Database

- The database contains the **mean values** and the **standard deviations** of different diagnostic measurements at each **plateau** (quasi-steady-state).
- The plateaus are identified intersecting the **total power plateaus** and the **plasma current plateaus**.
- There are **285** discharges with **732** plateaus in the database.

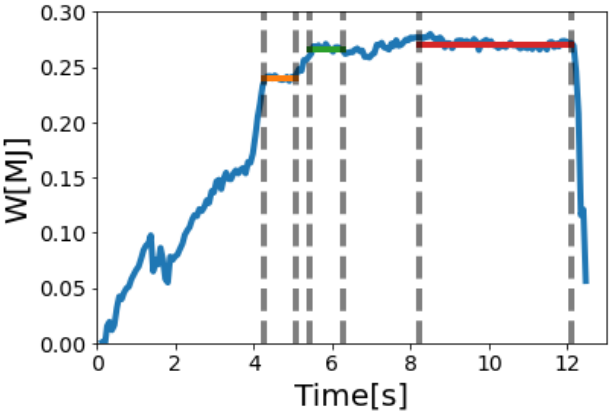

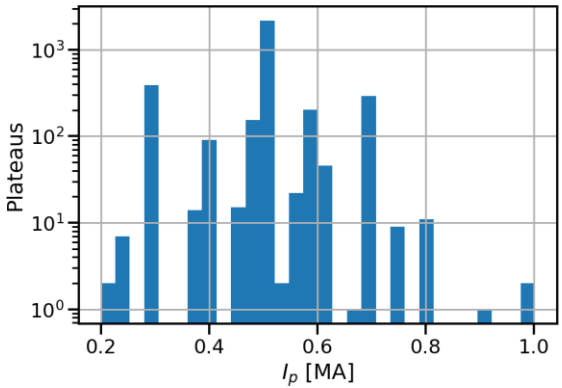

Two different confinement states coexist in WEST operation

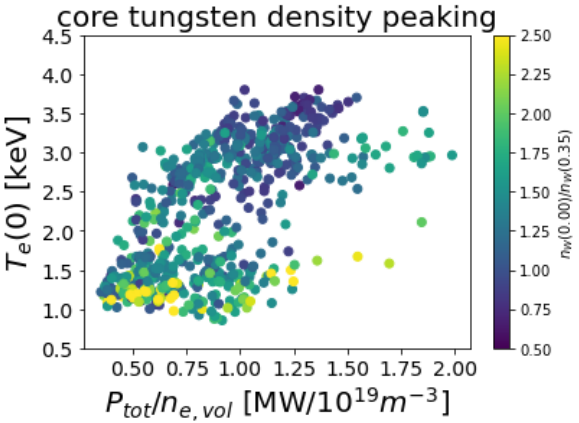

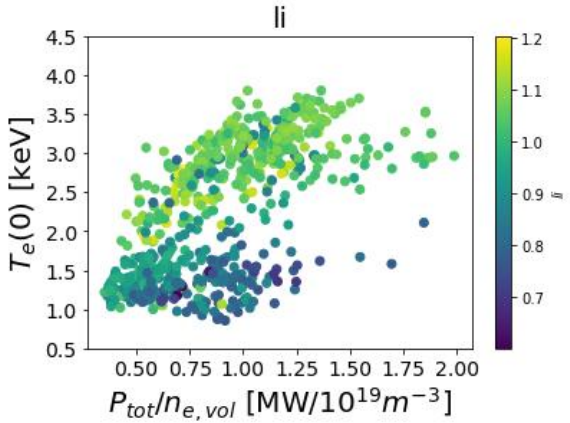

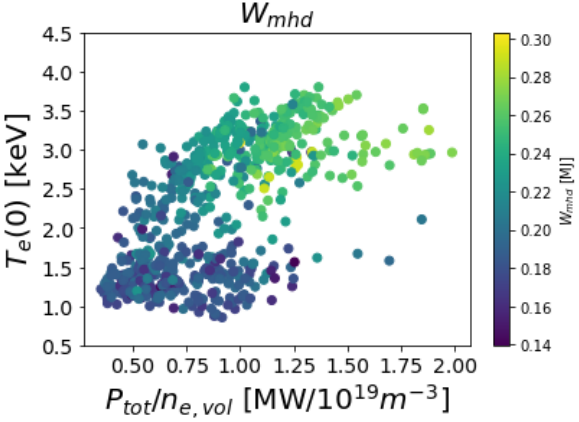

- $T_e\,(0)$ *and* W_{mhd} ↗
- *core tungsten peaking* ↘
- *li* ↗ ⇓
- *less prone to mhd activity*

Central electron temperature radiative collapse

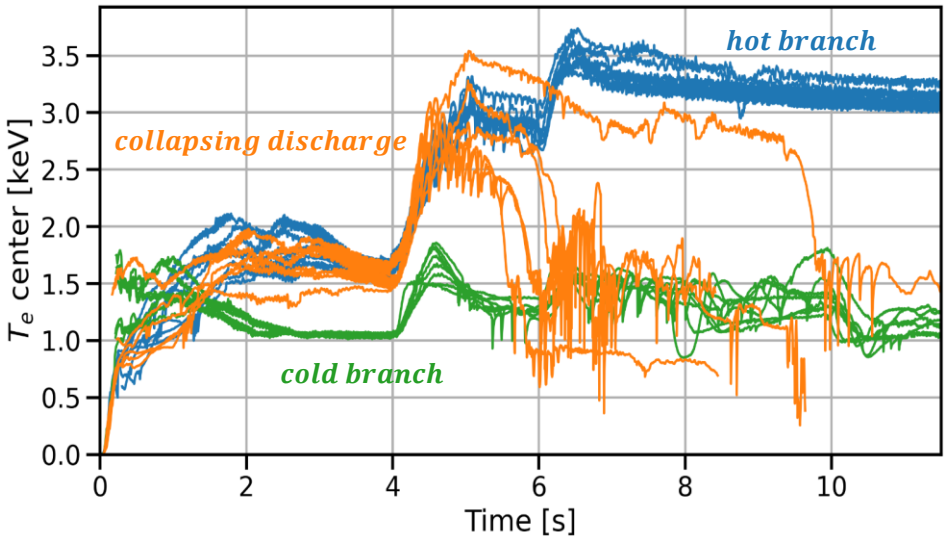

Some of the **hot branch** discharges go to the **cold branch** due to a **radiative collapse** of the central electron **temperature.**

Two questions arise from this analysis:

- Why are there two branches;
- Why the **25%** of the **discharges** in the hot branch **collapse.**

Outline

- Context;
- **Characterize and understand the dynamics of the radiative collapse observed in WEST operation;**
- Reproduce the rapid collapse of central temperature using an integrated model framework to understand which are the actuators that lead to the observed dynamics;
- Conclusions.

Characterizing the $T_e(0)$ dynamics in the database

Automatic identification of radiative collapses within plateaus:

$exponential\ fit: \boldsymbol{T_e(0) = -e^{(a+bt)} + c}$
$with\ \boldsymbol{a < 0}\ for\ the\ concavity,$

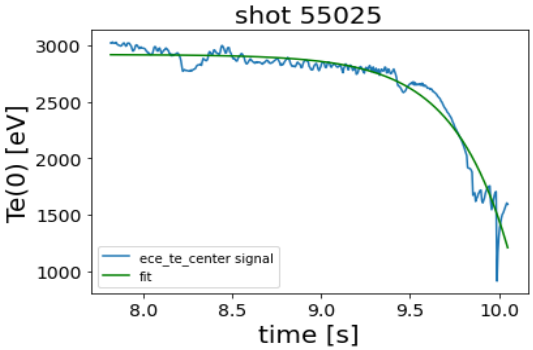

$linear\ function\ fit$
$with\ \boldsymbol{slope < -830}$

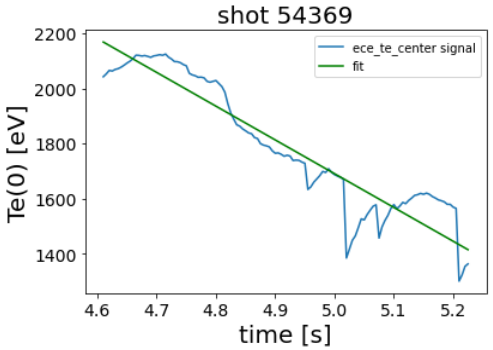

Three categories identified:
unstable plateaus where a collapse takes place, **cold stable plateaus** and remaining plateaus called **stable hot.**

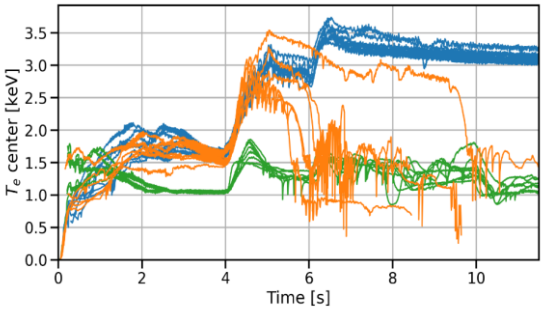

Unstable plateaus consistent with W cooling factor unstable range

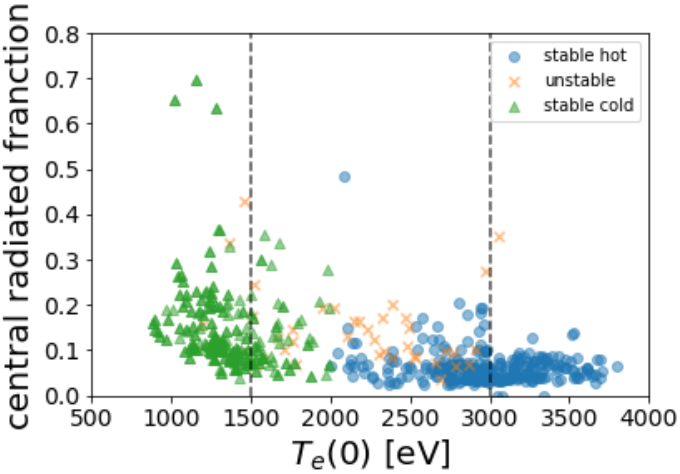

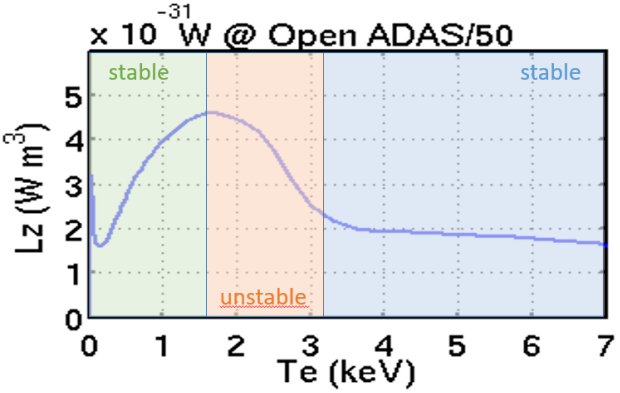

The **unstable plateaus** range between **1.5 keV** and **3 keV**. In this range, a **decrease** of electron **temperature** leads to an **increase** of **radiative losses** for the same **W content**.

25% of the **hot branch** is affected by a rapid **collapse** of the central electron temperature.

Collapsing discharge description

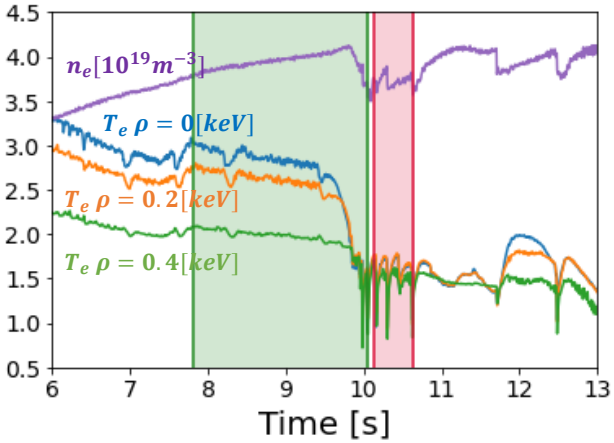

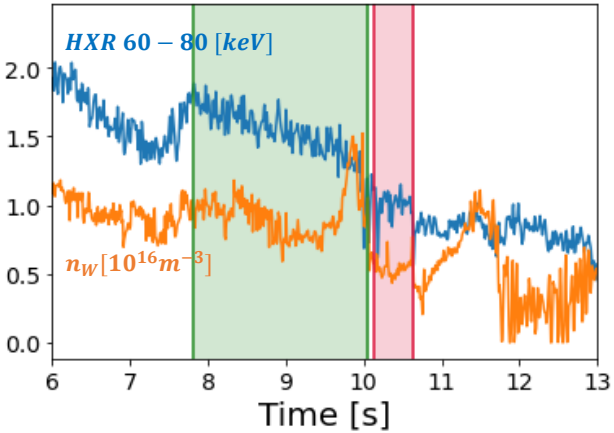

Prior to the collapse:

- a slow **increase** of **electron density;**
- a slow **decrease** of **electron temperature;**
- a **constant W** density;
- a slow **decrease** of central **HXR signal**: signature of a lower fast electron production by **LHCD.**

This complex interplay requires **integrated modelling.**

Outline

- Context;
- Characterize and understand the dynamics of the radiative collapse observed in WEST operation;
- **Reproduce the rapid collapse of central temperature using an integrated model framework to understand which are the actuators that lead to the observed dynamics;**
- Conclusions.

Integrated modelling settings

The 1D transport code **RAPTOR** is used to simulate the **collapse.** [F. Felici NF 2018]

The **transport coefficients** are computed using the **10D Neural Network version** trained on **QuaLiKiz**. [K. van de Plassche PP 2020]

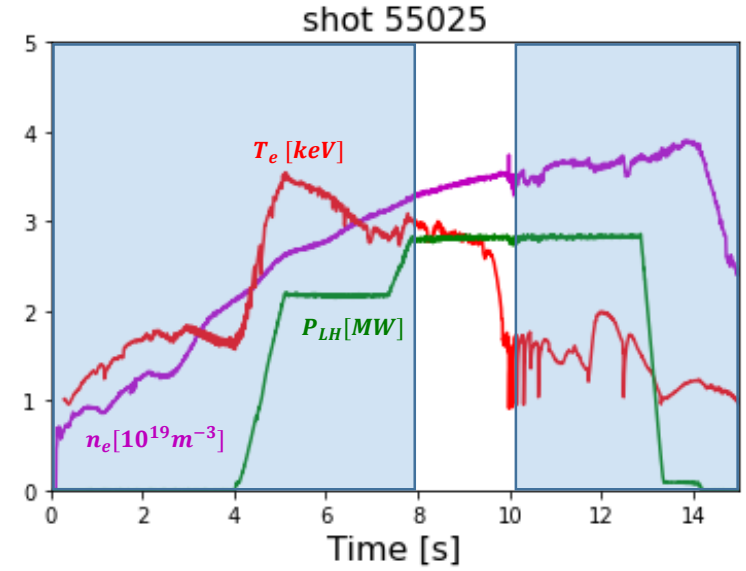

T_e and T_i	Predicted using QLKNN-10D
P_{LHCD}	LUKE [Peysson FST 2014]
n_e	interpretative
n_w	Interpretative, based on bolometry inversion
P_{rad}	Consistent with ADAS database
j(r)	predictive
equilibrium	Self-consistent inside a fixed LCFS

The $T_e(0)$ collapse is captured by the modelling

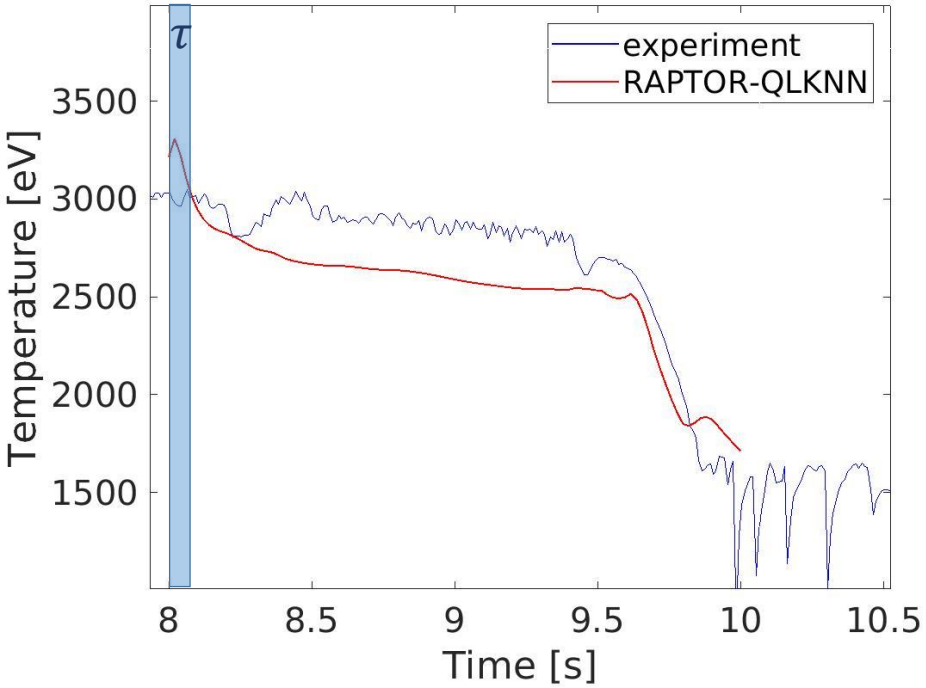

We will now investigate the role of two key ingredients: the **W profile evolution** and the **LHCD power absorption evolution.**

LHCD deposition is computed with the LUKE code [Peysson FST 2014]

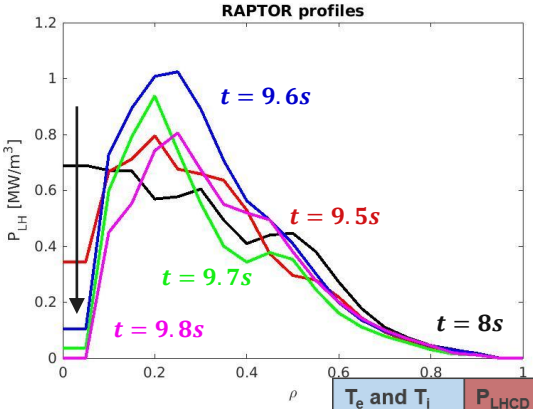

The **power deposition** in the very **core cannot be computed** with the required spatial accuracy. The **central value is adjusted** in time **to match the temperature** evolution.

A progressive **decrease** of the core electron heating by **LHCD** occurs during the slow density rise. Then it is **amplified** before the **radiative collapse**.

T_e and T_i	P_{LHCD}	n_e	n_w	P_{rad}	j(r)	equilibrium
Predicted using QLKNN-10D	LUKE	interpretative	Interpretative, based on bolometry inversion	ADAS	predictive	Self-consistent inside a fixed LCFS

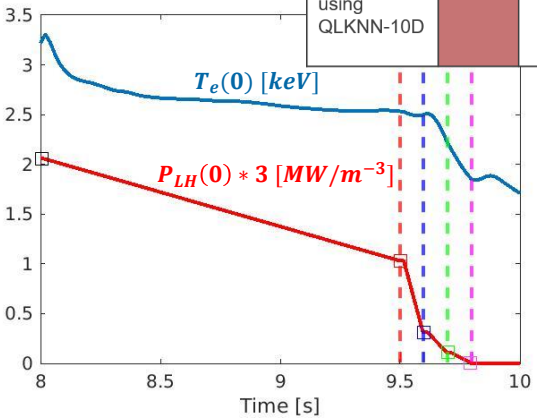

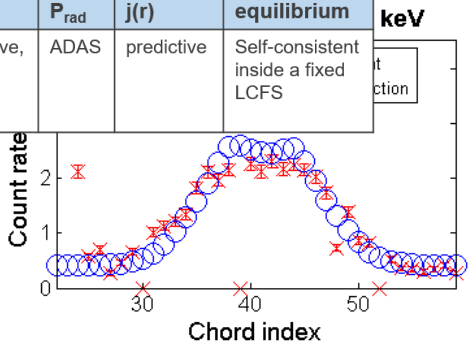

W profile obtained using bolometry measurements

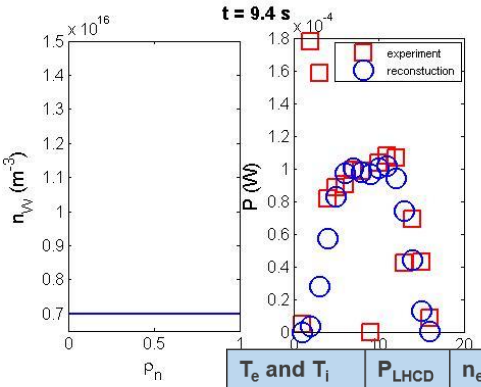

It has been assumed that n_W can be approximated by a **Gaussian symmetric** to the center of the plasma **on top of a flat profile**.

The 16 horizontal **bolomery chords** are used **to constrain the W profile** for T_e>1keV only, where the L_W are known.

T_e and T_i	P_{LHCD}	n_e	n_w	P_{rad}	j(r)	equilibrium
Predicted using QLKNN-10D	LUKE	interpretative	Interpretative, based on bolometry inversion	ADAS	predictive	Self-consistent inside a fixed LCFS

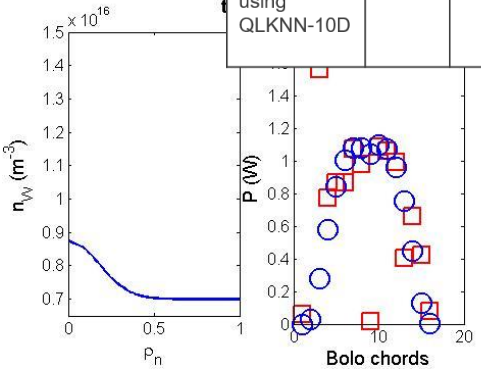

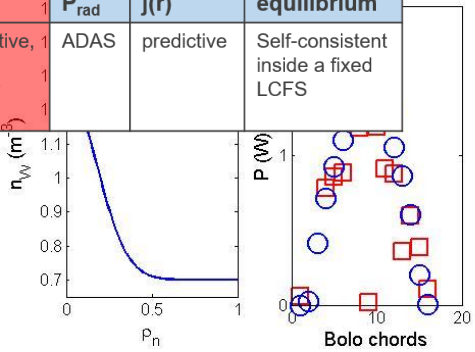

W peaking during central T_e collapse captured by reduced neoclassical T_i screening

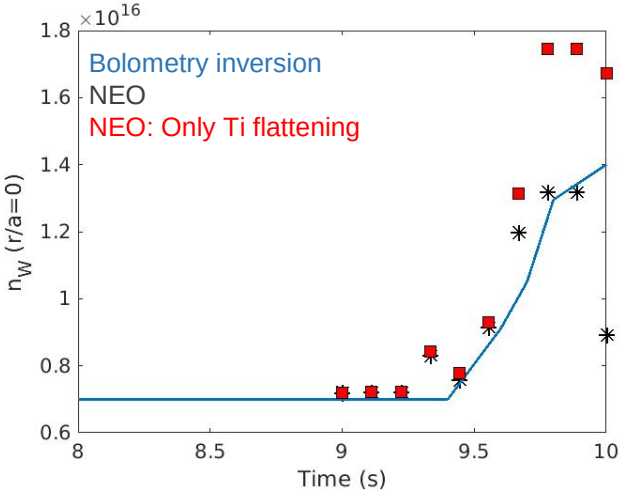

Neoclassical and turbulent transport computed with NEO [Belli 2008]

Tungsten density reconstructed from transport coefficients (BC at r/a=0.3)

In very good quantitative agreement with bolometry inferred tungsten density

W peaking increases strongly due to a core **T_e flattening**, leading to **T_i flattening** by equipartition, hence **reducing** the neoclassical **T screening effect.**

Tungsten peaking and LHCD core absorption reduction are both needed for the collapse

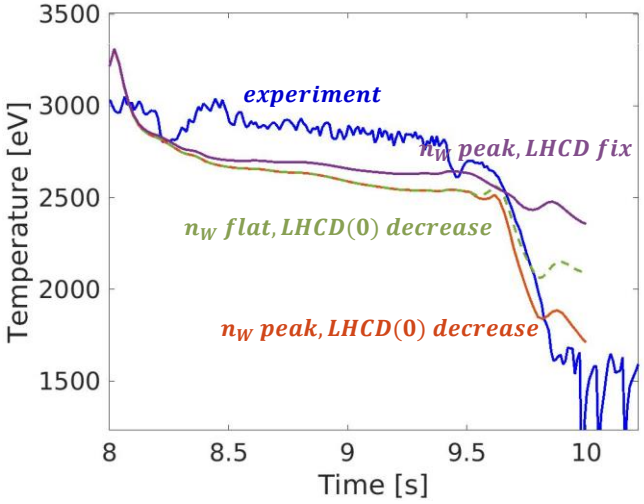

The **collapse** is not reproduced if the **radiated power** inside ρ=0.1 does not **overtake the central electron heating**. If core radiative fraction exceeds 1 the collapse occurs.

Only with both the contribution of the **tungsten accumulation** and the **decrease of** the central **LHCD** injection the **speed of collapse is reproduced.**

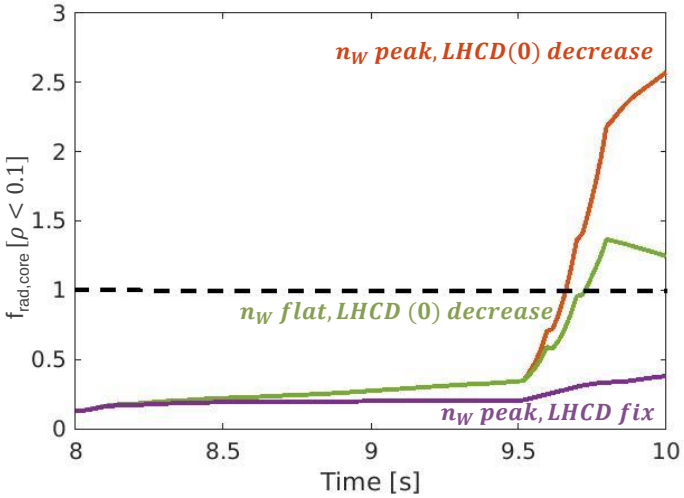

Collapse reproduction in discharge 54802

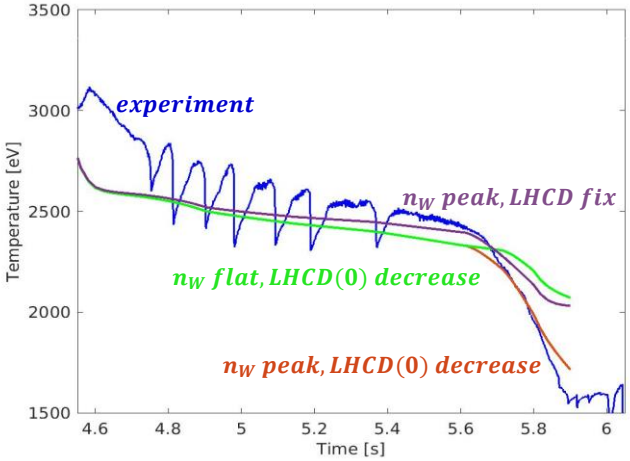

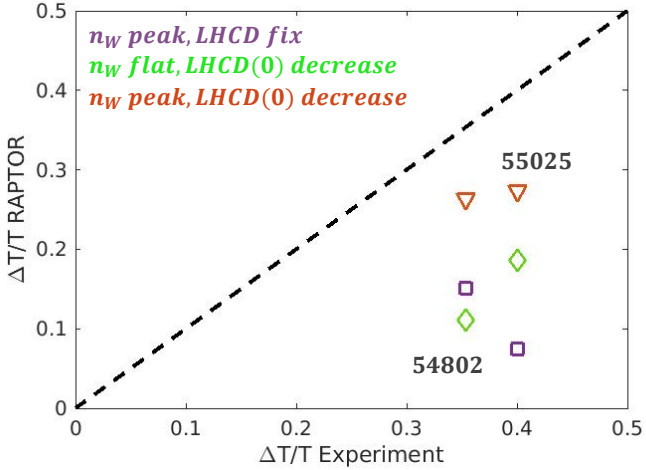

The same procedure was carried out for the **54802 discharge**.

The temperature collapses are associated to **variable contributions** of **LHCD** core heating depletion and **tungsten peaking**.

Outline

- Context;
- Characterize and understand the dynamics of the radiative collapse observed in WEST operation;
- Reproduce the rapid collapse of central temperature using an integrated model framework to understand which are the actuators that lead to the observed dynamics;
- **Conclusions.**

Conclusions

- In the database, L mode **plateaus** where $T_e(0)$ rapidly **collapse** are identified in the range of **1.5 keV** and **3 keV,** consistent with **tungsten cooling factor**.
- Time sequence of $T_e(0)$ collapse acceleration:
  - The **slight density rise** leads to **less on-axis LHCD power deposition** enhancing the central **T_e reduction**;
  - **T flattening** in core leads to a **reduction of W core temperature screening** hence **core W accumulation**
- Core **electron heating is essential** in a **W environment**.

Note: ECRH will be installed on WEST in 2023 to mitigate core LHCD deposition sensitivity

DE LA RECHERCHE À L'INDUSTRIE

BACK UP SLIDES

H_{WEST} for quantifying the quality of the confinement time

$$\tau_{mhd,measured} = \frac{W_{mhd}}{P_{tot}} = \frac{\frac{3}{2}\int_V P\, dV}{P_{ohmic} + P_{aux}} \rightarrow H_{WEST} = \frac{\tau_{mhd,measured}}{\tau_{scaling}}$$

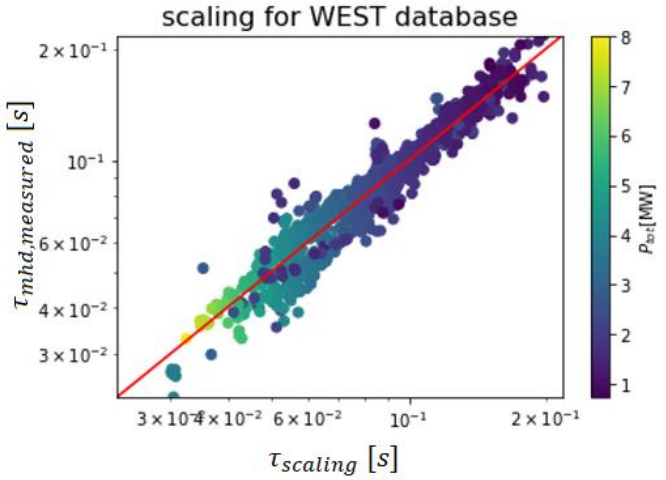

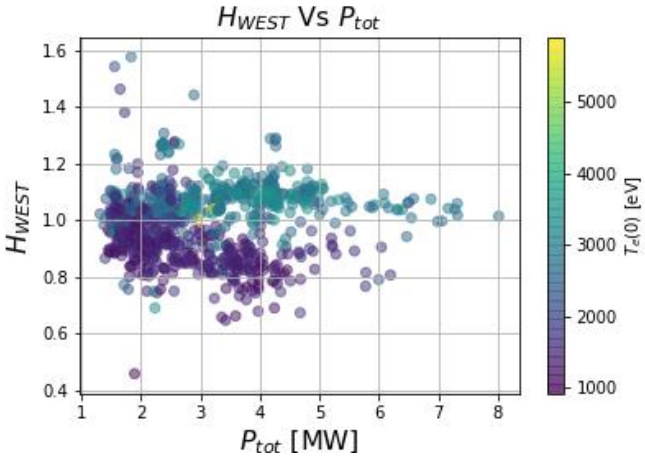

WEST database aligned with ITER96L

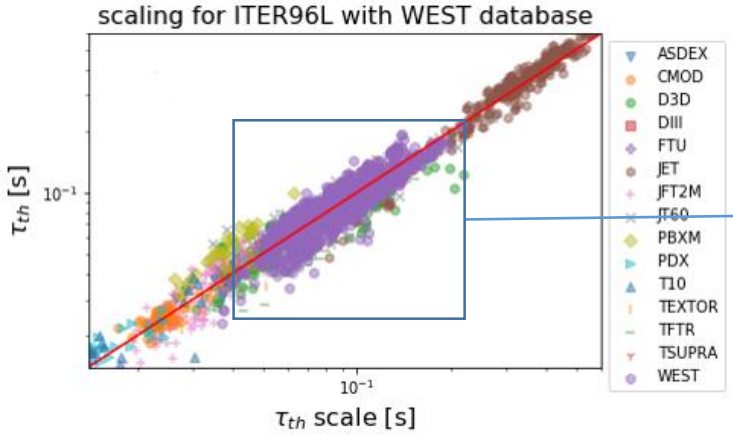

Filter:

- Small reconstruction errors;
- Diverted plasma;
- L-mode plateaus;
- LSN
- Only deuterium shots

$$\tau = C\, Ip^{\alpha_{Ip}} B^{\alpha_B} P_{tot}^{\alpha_P} n_e^{\alpha_{ne}} M^{\alpha_M} R^{\alpha_R} \varepsilon^{\alpha_\varepsilon} k^{\alpha_k}$$

$$\alpha_{Ip} = 1.35$$
$$\alpha_{n_e} = -0.16$$
$$\alpha_{P_{tot}} = -0.75$$

$$\tau_{scaling}$$

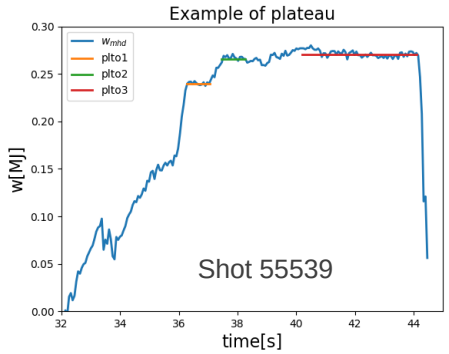

Bolometry tomography to compute the power emission density profile

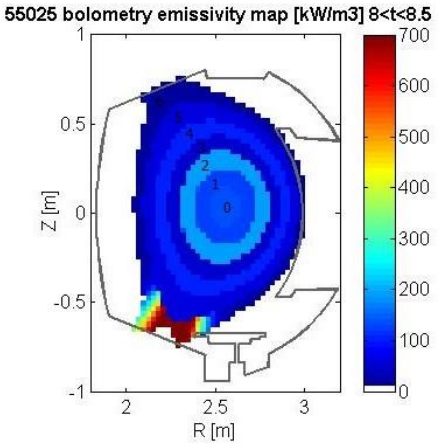

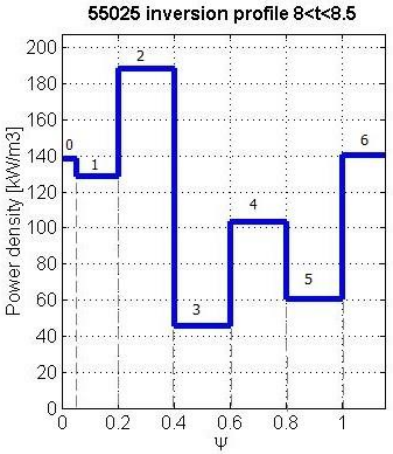

A **bolometer** measures a line-integrated value of the **local radiative emissivity** along a viewing line of sight.

A **concentric layer decomposition** of local plasma emissivity is assumed together **with asymmetric factors** in the SOL and edge. The tomography inversion is computed.

The **power emission** in $\frac{W}{m^3}$ **for each layer** are estimated.

Tungsten density profiles from the inverse of bolometry

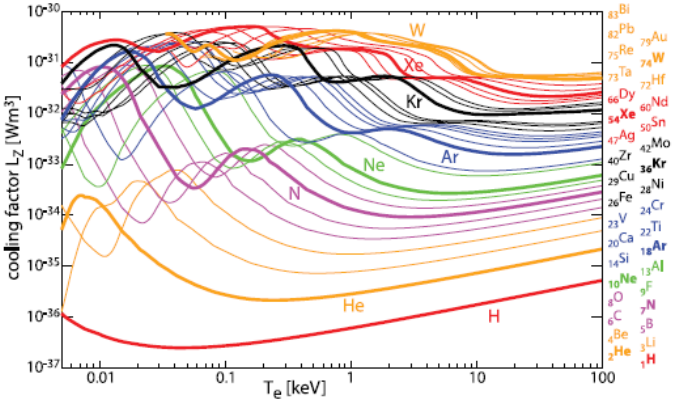

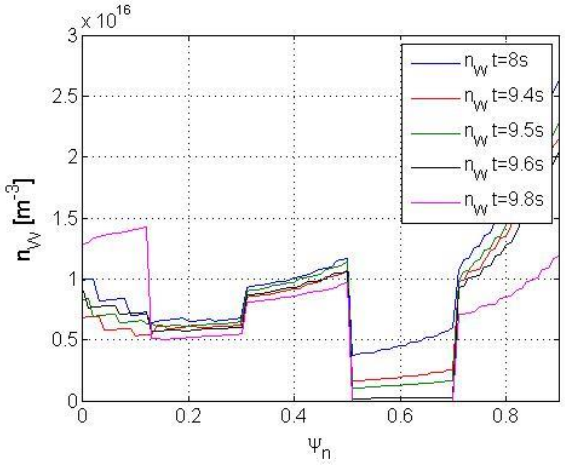

Above **1KeV** the **main radiator** is the **tungsten**.

Assuming that all the **emission radiation** comes from the **tungsten**, it is possible to use the inverse of bolometry to compute **its density** at each layer.

$$n_W \approx \frac{P_{rad,W}}{n_e L_W(T_e)}$$

$\frac{P_{tot}}{n_{e,vol}}$ for hot and cold branches and collapsing discharges

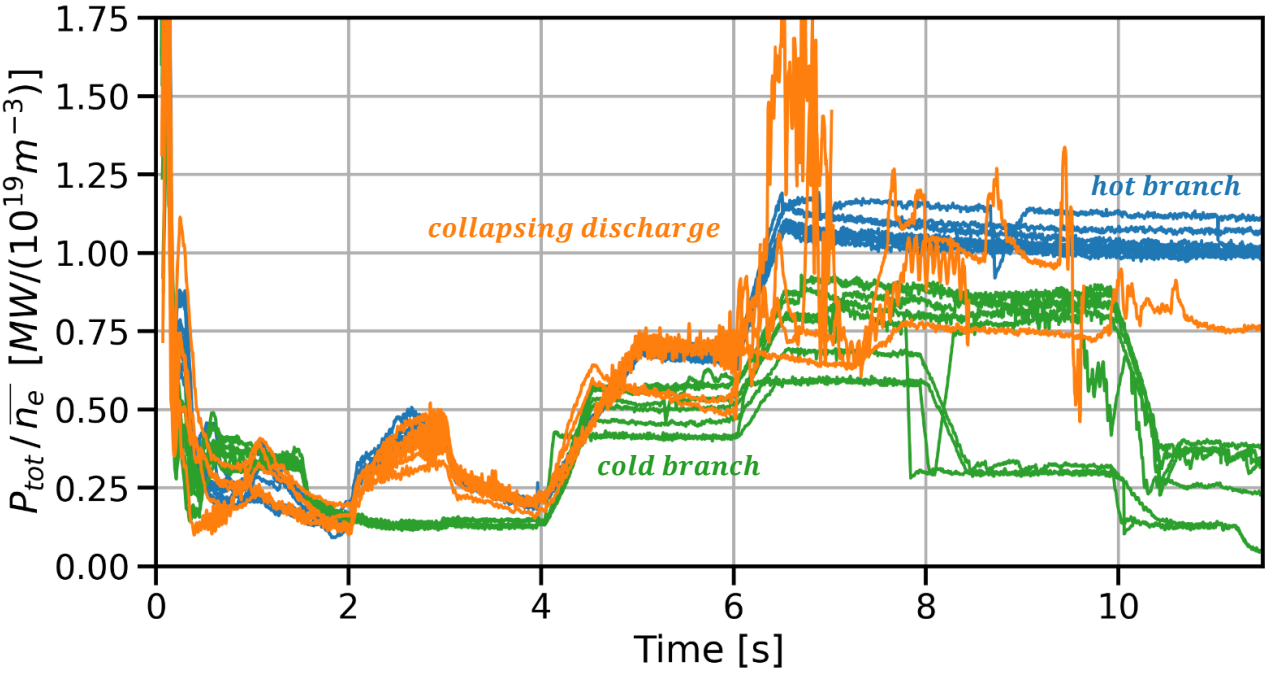

P_{LH} and $n_{e,vol}$ for hot and cold branches and collapsing discharges

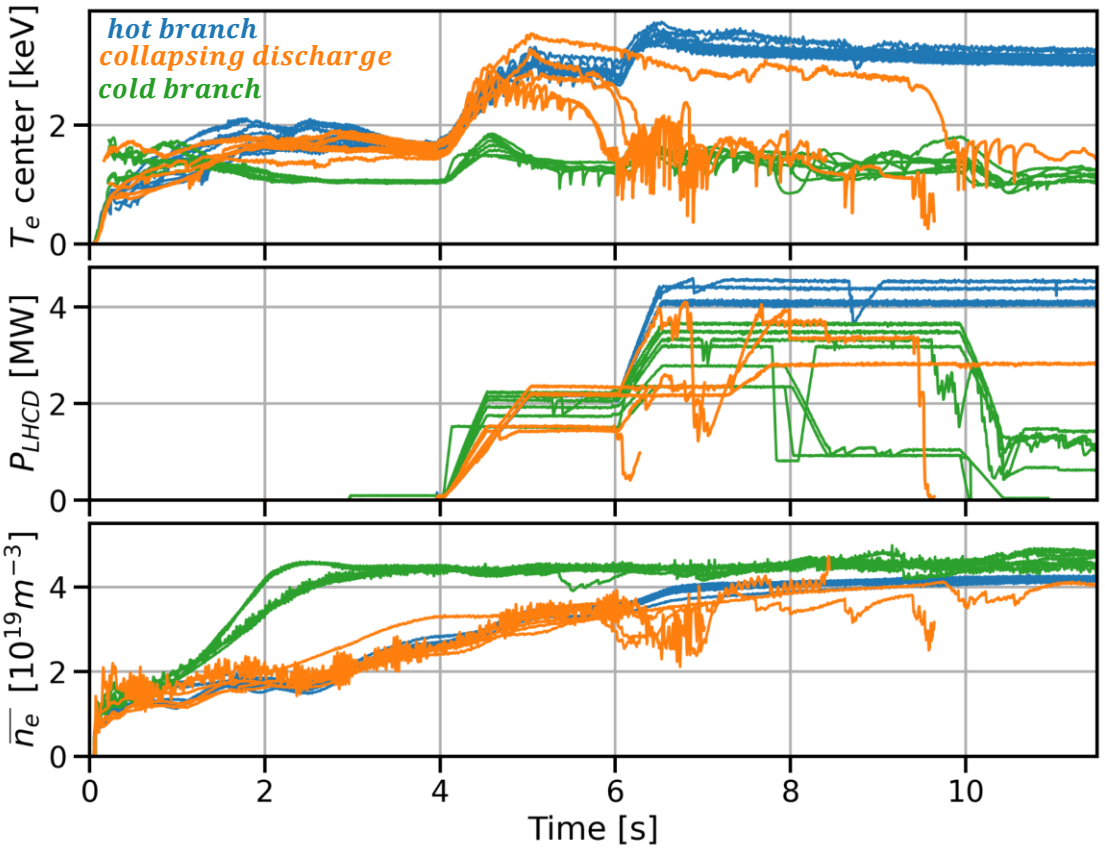

The T_e collapse is captured by the modelling

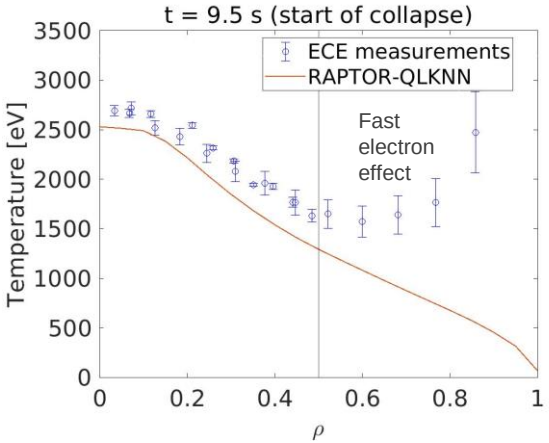

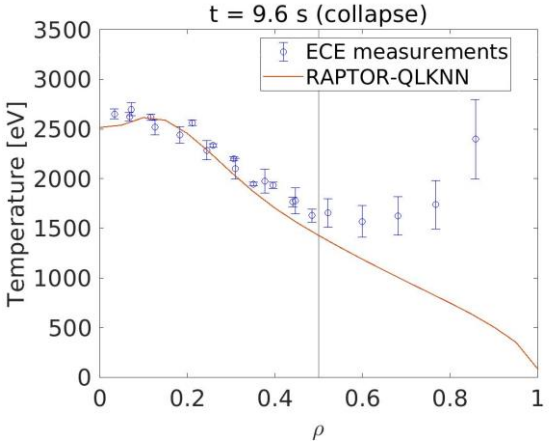

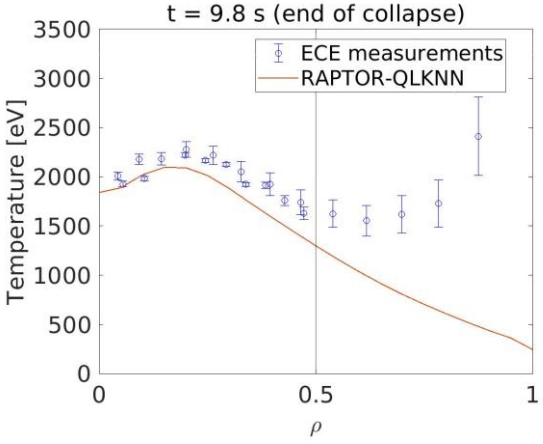

W neoclassical transport

W neoclassical transport (in absence of poloidal asymmetries)

$$\Gamma_W = -Zq^2 D n_W \left[\frac{1}{Z}\frac{\nabla n_W}{n_W} - \frac{\nabla n_i}{n_i} + \frac{1}{2}\frac{\nabla T_i}{T_i}\right]$$

Diffusion

Convection due to ion density peaking **(inward)**

Convection due to ion **thermal screening, outward**

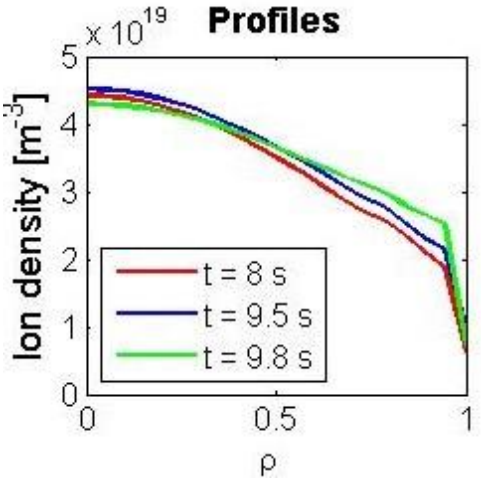

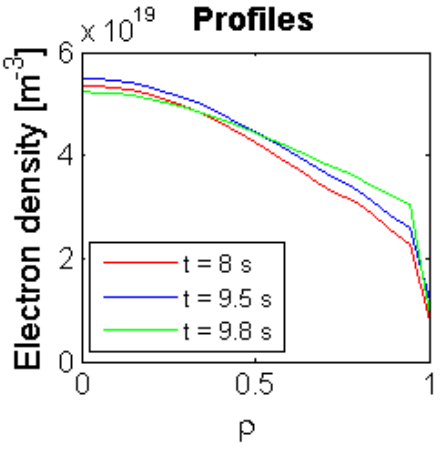

H mode

The plateaus in H mode in C4:

- In USN 4 plateaus
- In LSN 10 plateaus

Max duration of H mode on WEST 4 s.

The transitions are observed in the hot and cold branches.

The transitions are unstable because P_{rad} increases when the pedestal is formed and so the power that crosses the separator is reduced and we go back to L mode.

In C6 we will raise the density to high power because we think we were on the low density branch of the L-H transition.